Even-Skipped[+] Interneurons Are Core Components of a Sensorimotor Circuit that Maintains Left-Right Symmetric Muscle Contraction Amplitude

Highlights

- New model system for analysis of bilaterally symmetric motor output

- Identify a role for the conserved Eve[+] interneurons in locomotor behavior

- Imaging of neural activity in an intact, freely moving *Drosophila* larvae

- Identify a multisynaptic sensorimotor circuit using TEM reconstruction

Authors

Ellie S. Heckscher, Aref Arzan Zarin, Serge Faumont, ..., Albert Cardona, Shawn R. Lockery, Chris Q. Doe

Correspondence

heckscher@uchicago.edu (E.S.H.), cdoe@uoregon.edu (C.Q.D.)

In Brief

During symmetrical motor activities— e.g., breathing, whisking, and hopping— bilateral pairs of muscles contract synchronously and with equal amplitude. Heckscher et al. identify the evolutionarily conserved Eve[+] interneurons as part of a sensorimotor circuit that maintains symmetric bilateral muscle contraction amplitude.

CrossMark

Even-Skipped+ Interneurons Are Core Components of a Sensorimotor Circuit that Maintains Left-Right Symmetric Muscle Contraction Amplitude

Ellie S. Heckscher,[1,2,3,6,*] Aref Arzan Zarin,[1,2,3] Serge Faumont,[1] Matthew Q. Clark,[1,2,3] Laurina Manning,[1,2,3] Akira Fushiki,[4] Casey M. Schneider-Mizell,[4] Richard D. Fetter,[4] James W. Truman,[4] Maarten F. Zwart,[4,5] Matthias Landgraf,[5] Albert Cardona,[4] Shawn R. Lockery,[1] and Chris Q. Doe[1,2,3,*]

[1]Institute of Neuroscience, University of Oregon, Eugene, OR 97403, USA
[2]Institute of Molecular Biology, University of Oregon, Eugene, OR 97403, USA
[3]Howard Hughes Medical Institute, University of Oregon, Eugene, OR 97403, USA
[4]Janelia Research Campus, HHMI, Ashburn, VA 20147, USA
[5]Department of Zoology, University of Cambridge, Cambridge CB2 3EJ, UK
[6]Present address: Department of Molecular Genetics and Cell Biology, University of Chicago, Chicago, IL 60637, USA
*Correspondence: heckscher@uchicago.edu (E.S.H.), cdoe@uoregon.edu (C.Q.D.)
http://dx.doi.org/10.1016/j.neuron.2015.09.009

SUMMARY

Bilaterally symmetric motor patterns—those in which left-right pairs of muscles contract synchronously and with equal amplitude (such as breathing, smiling, whisking, and locomotion)—are widespread throughout the animal kingdom. Yet, surprisingly little is known about the underlying neural circuits. We performed a thermogenetic screen to identify neurons required for bilaterally symmetric locomotion in *Drosophila* larvae and identified the evolutionarily conserved Even-skipped+ interneurons (Eve/Evx). Activation or ablation of Eve+ interneurons disrupted bilaterally symmetric muscle contraction amplitude, without affecting the timing of motor output. Eve+ interneurons are not rhythmically active and thus function independently of the locomotor CPG. GCaMP6 calcium imaging of Eve+ interneurons in freely moving larvae showed left-right asymmetric activation that correlated with larval behavior. TEM reconstruction of Eve+ interneuron inputs and outputs showed that the Eve+ interneurons are at the core of a sensorimotor circuit capable of detecting and modifying body wall muscle contraction.

INTRODUCTION

Bilaterally symmetric motor patterns—those in which muscle contractions on the left and right sides of the body occur synchronously and with equal amplitude—are widespread throughout the animal kingdom. They regulate respiration, speech, smiling, whisking, flight, and various locomotor gaits. Surgical manipulations in both vertebrates and invertebrates have shown that contralaterally projecting commissural interneurons are required for bilaterally symmetric motor output,

demonstrating that symmetric motor output is not merely a default state (Dubayle and Viala, 1996; Jahan-Parwar and Fredman, 1980; Lanuza et al., 2004; Murchison et al., 1993; von der Porten et al., 1982). In the mouse, genetic deletion of the Dbx1+ transcription factor from V0 interneurons disrupted left-right synchronous motor output during respiration and caused perinatal lethality (Bouvier et al., 2010). Loss of the *dbx1* locus affected both ventral Evx1+ interneurons and dorsal Evx1− interneurons, whereas a more specific loss of just the dorsal Dbx1+ interneurons had no effect on breathing. Taken together, these data implicate Evx1+ interneurons in regulating respiratory motor rhythms (Bouvier et al., 2010). However, this interpretation is clouded by the observation that Evx1 knockout mice appear to breathe normally, despite any detectable Evx1 or Evx2 protein in V0 interneurons (Moran-Rivard et al., 2001). These findings demonstrate how little we understand about the molecules and neural circuitry underlying bilaterally symmetric motor output, despite its broad and essential functions.

Drosophila larval crawling is a genetically tractable model system for investigating the molecular and neuronal underpinnings of symmetric motor output. Larval crawling is a simple, robust motor behavior that involves waves of rhythmic, bilaterally symmetric body wall muscle contractions (Heckscher et al., 2012). The segmented larva has ∼30 bilateral body wall muscles per segment and a similar number of motor neurons, and their role during larval locomotion has been characterized (Berni et al., 2012; Crisp et al., 2008, 2011; Dixit et al., 2008; Heckscher et al., 2012; Hughes and Thomas, 2007; Lahiri et al., 2011; Pulver and Griffith, 2010; Schaefer et al., 2010). In contrast, there are ∼270 bilateral interneurons per segment (Heckscher et al., 2014; Rickert et al., 2011), and their role in locomotion is almost completely unknown (Kohsaka et al., 2014). Recently, we identified several hundred Gal4 lines that express in a sparse pattern of neurons in the late embryonic CNS and determined their expression pattern at single neuron resolution for 75 of these lines (Heckscher et al., 2014; Manning et al., 2012). We used this collection of sparsely expressed Gal4 lines to express the warmth-activated TRPA1 cation channel and screen for
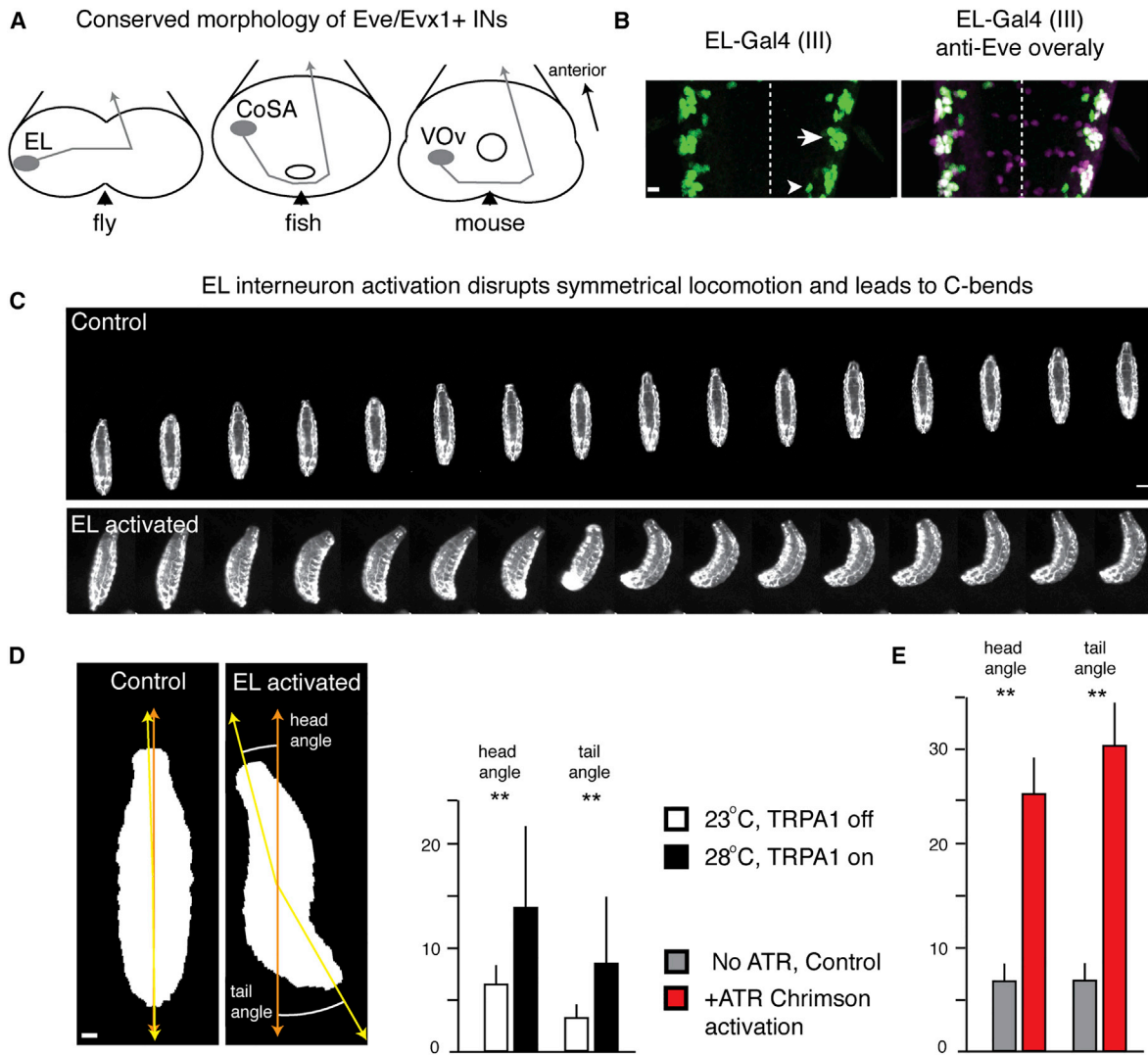
Figure 1. Activation of EL Interneurons Causes Larval Crawling Defects

(A) Eve/Evx1^{+} interneurons have commissural ascending axons in flies, fish, and mouse (midline, black arrowheads and anterior, up in all figures unless noted).

(B) *EL-gal4* (green) is consistently in nine ELs (arrow) and stochastically in few Eve-negative non-ELs (arrowhead) (Eve protein, magenta) (colocalization with *EL-gal4*, white) (midline, dashed). The scale bar represents 10 μm (genotype: *EL-gal4 / UAS-nls-GFP*).

(C) Activation of ELs reduces larval crawling speed and induces C-bends. The frames are shown at 0.5 s intervals. The scale bar represents 150 μm (genotype: *UAS-dTRPA1/+; EL-gal4(III)/EL-gal4(III)*) (Control: 23°C, TRPA1 off and EL activated: 28°C, TRPA1 on).

(D) TRPA1 activation of ELs results in larval C-bends with laterally displaced head and tail; genotype as in (C). See Movies S1 and S2. The scale bar represents 40 μm. The average and SEM are shown (**p < 0.05 and t test).

(E) Chrimson activation of ELs results in larval C-bends with laterally displaced head and tail (genotype: *UAS-Chrimson.mVenus/+; EL-gal4(III)/+*) (Control: larvae raised on food without ATR and EL activated: raised on food with ATR). See Movies S3 and S4. The average and SEM are shown (**p < 0.05 and t test).

locomotor defects in newly hatched larvae. We identified a small pool of interneurons ("ELs") that express the evolutionarily conserved transcription factor Even-skipped (Eve; Evx1/2 in mammals) that are required to maintain bilaterally symmetric motor output.

Eve/Evx[+] interneurons are found in the nerve cord of almost all bilateral animals examined to date, including annelids, chordates, insects, fish, birds, and mammals, as well as a proposed common ancestor between invertebrates and vertebrates, *Platy-nereis dumerilii* (Avaron et al., 2003; Copf et al., 2003; Denes et al., 2007; Ferrier et al., 2001; Holland, 2013; Ikuta et al., 2004; Moran-Rivard et al., 2001; Sordino et al., 1996; Takatori et al., 2008; Thaëron et al., 2000). In all cases where the morphology of Eve/Evx[+] interneurons has been examined, they have contralateral ascending projections, such as the zebrafish CoSA and mouse V0v interneurons (Figure 1A) (Moran-Rivard et al., 2001; Suster et al., 2009). In flies, Eve is expressed in segmentally reiterated subsets of interneurons and motor

neurons, but not in the brain (Figure S1) (Frasch et al., 1987). The Eve/Evx transcription factor is well known to specify neuronal identity and regulate axon pathfinding in fly and worm motor neurons as well as in mammalian interneurons (Broihier and Skeath, 2002; Doe et al., 1988; Esmaeili et al., 2002; Fujioka et al., 2003; Landgraf et al., 1999; Moran-Rivard et al., 2001; Zarin et al., 2014). However, despite years of intense study, the behavioral role of the Eve/Evx+ interneurons remains poorly defined. Our results show that the Eve+ interneurons are part of a sensorimotor circuit that maintains left-right symmetry of muscle contraction amplitude in *Drosophila* larvae.

RESULTS

The EL Interneurons Maintain Left-Right Symmetric Larval Locomotion

To identify the interneurons required for larval locomotion, we used a collection of Gal4 lines that sparsely label neurons in the late embryonic CNS (Heckscher et al., 2014; Manning et al., 2012) to express the warmth-activated cation channel TRPA1 (Pulver et al., 2009) and screened for defects in larval locomotion. We screened newly hatched larvae for locomotor defects following activation of TRPA1 (28°C) that were reversed following inactivation of TRPA1 (23°C). Here, we focus on the evolutionarily conserved Eve+ lateral (EL) interneurons that are specifically targeted by the *EL-gal4* line (Figure 1B) (Fujioka et al., 1999).

Wild-type first instar larvae crawl with a linear posture at both 23°C and 28°C (data not shown), as do larvae expressing TRPA1 in the ELs at 23°C (Figure 1C, top, and Movie S1; Table S1). In contrast, raising the temperature to 28°C to induce TRPA1 stimulation of the ELs resulted in slower crawling and abnormal left-right asymmetric body posture, which we call "C-bends" (Figures 1C and 1D and Movie S2; Table S1). Similarly, Chrimson optogenetic stimulation of ELs resulted in pronounced C-bends (Figure 1E and Movies S3 and S4). C-bends are different from normal larval turning because they can occur in posterior segments, whereas larval turning is performed by anterior segments (Berni, 2015; Lahiri et al., 2011). We conclude that bilateral activation of EL interneurons is sufficient to disrupt left-right symmetric body posture.

We tested next whether the ELs were required for left-right symmetric locomotion. We used *EL-gal4* to express the pro-apoptotic Hid/Reaper proteins, which typically removed all but 1–2 ELs per hemisegment (Figure 2A). Similar to EL activation, ablation of the ELs led to slow crawling speeds and "wavy" body posture, including C-bends (Figures 2B–2E and Movie S5). Because ablation removes statistically similar numbers of ELs from the left and right sides of the nerve cord (Figure 2A), and because C-bends can occur in both directions within the same animal (Figure 2C), we conclude that bilateral ablation leads to a randomized left-right asymmetric body posture.

Although EL interneurons are present only in the nerve cord, the *EL-gal4* line is stochastically expressed in a few cells in the brain (Figure S1). To test whether ablation of these neurons caused locomotor defects, we used *tsh-gal80* (Clyne and Miesenböck, 2008) to inhibit *EL-gal4* in the nerve cord, but not in the brain. We found that ablation of the *EL-gal4* neurons in only the brain had no defects in locomotion (Figure 2E). We conclude that the Eve+ ELs within the nerve cord are required for bilaterally symmetric crawling in *Drosophila* larvae, and that the normal function of EL interneurons is to maintain left-right symmetric muscle contractions during linear locomotion.

EL Interneurons Maintain Left-Right Symmetric Muscle Contraction Amplitude without Affecting Contraction Timing

To determine how the EL interneurons regulate motor output, we quantified muscle contraction timing in wild-type, EL ablated, and EL activated larvae. We found that all genotypes showed left-right synchronous muscle contractions (Figures 3A–3C; Table S2). The lack of effect on muscle contraction timing suggests that the ELs are not part of the central pattern generator (CPG), addressed in more detail below. We conclude that EL interneurons are not required for left-right synchronous timing of muscle contraction.

We next measured left-right muscle resting length and maximum contraction amplitude. Control larvae showed bilateral symmetry in resting muscle length and maximum contraction amplitude (Figure 3A and Movie S6; Table S2). In contrast, both EL ablated and EL activated larvae showed significant left-right differences in resting muscle length and maximum muscle contraction amplitude during forward locomotion (Figures 3B and 3C and Movies S7 and S8; Table S2). The resting muscle phenotype is consistent with our observations that EL disruption can create left-right asymmetry in larvae at rest (data not shown). We conclude that the EL interneurons are required for maintaining bilaterally symmetric muscle contraction amplitude, both at rest and during active muscle contraction.

Calcium Imaging Reveals Functional Interactions among EL Interneurons

To better understand the neural circuit containing the EL interneurons, we asked if the ELs could be part of the CPG for locomotion. We performed calcium imaging in the isolated CNS, which lacks all sensory input, and asked if ELs showed locomotion-like patterns of activity. As a positive control, we confirmed that motor neurons show locomotion-like posterior to anterior waves of activity (Figure S2 and Movie S9) as has been previously reported (Pulver and Griffith, 2010; Schaefer et al., 2010). In contrast, the ELs showed only spontaneous activity in individual neurons (Figure S2 and Movie S10). We conclude that the EL interneurons are neither part of the locomotor CPG, nor receive input from the locomotor CPG.

Next, to understand how TRPA1-induced stimulation of EL interneurons could lead to a behavioral phenotype, we asked how the EL interneurons themselves responded to bilateral activation. We used TRPA1 to chronically stimulate EL interneurons, similar to our behavioral experiments, and monitored EL activity using the calcium sensor GCaMP6m. Imaging was done in the isolated CNS to reduce movement artifacts and eliminate sensory input (Figure 4A). We observed three types of response. Most commonly, the EL interneurons were strongly activated on one side of the CNS and weakly activated on the other side; at stimulus offset the response reliably switched sides (Figures 4A–4C, group 1, n = 10, and Movie S11). This left-right
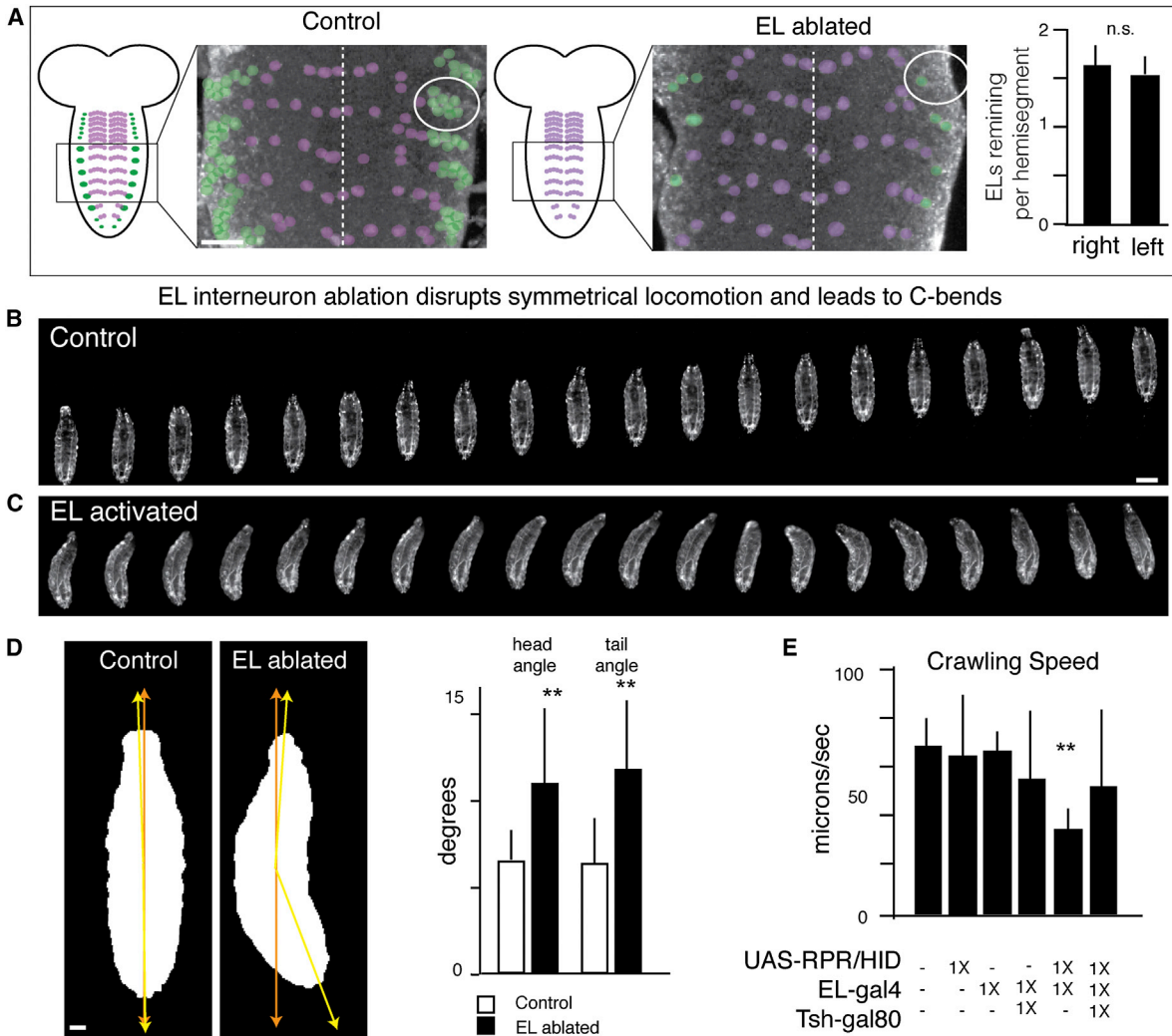
Figure 2. Ablation of EL Interneurons Causes Larval Crawling Defects

(A) L1 CNS stained for Eve protein, with the focal plane showing a subset of Eve^{+} motor neurons (pseudocolored magenta) and the lateral cluster of Eve[+] EL interneurons (pseudocolored green). The EL ablation reduces EL number from ~10 to 1.63 ± 0.21 (left) and 1.54 ± 0.19 (right). The left-right difference is not significant (t test and n = 4 larvae). The scale bar represents 10 μm. (Control genotype: *UAS-reaper, UAS-hid / Y* and EL ablated genotype: *UAS-reaper, UAS-hid / Y;;EL-gal4/+*).

(B–D) Ablation of ELs decreases larval crawling speed and induces C-bends. The genotypes are as in (A).

(B and C) Frames are shown at 0.5 s intervals. The scale bar represents 150 μm.

(D) The scale bar represents 40 μm. The average and SEM are shown (**p < 0.05 and t test). See Movie S5.

(E) EL-gal4^{+} brain neurons are not required for normal locomotion, genotypes from left: (1) y w; (2) UAS-reaper, UAS-hid / Y; (3) EL-gal4 (III)/+; (4) UAS-reaper, UAS-hid /Y;;EL-gal4 /+; (5) tsh-Gal80/+; EL-gal4 /+; and (6) UAS-reaper, UAS-hid /Y; tsh-Gal80/+; EL-gal4 /+ (in this genotype only EL-gal4^{+} neurons in the brain are ablated).

(B, D, and E) Average and SEM shown (**p < 0.05 and t test).

asymmetric response to presumably bilaterally symmetric TRPA1 activation suggests that left-right EL interneurons exhibit functional interactions. Less commonly, we observed bilaterally symmetrical activity that was low during stimulation and increased at stimulus offset (Figures 4B and 4C, group 2, n = 6) or EL activity mirroring TRPA1 activity (Figures 4B and 4C, group 3, n = 6), the response expected if the ELs had no functional interactions. For all groups, once the pattern of EL activity was established, it remained constant for the duration of the

chronic TRPA1 stimulation interval; this is in contrast to EL activity within intact larvae (see next section). We conclude that there can be functional interactions between left-right EL interneurons.

Calcium Imaging of EL Activity within Intact Freely Moving Larvae Provide Functional Evidence that the EL Interneurons Are Part of a Sensorimotor Circuit

We wanted to understand how EL interneurons respond to stimulation in vivo, and whether EL response is correlated with larval
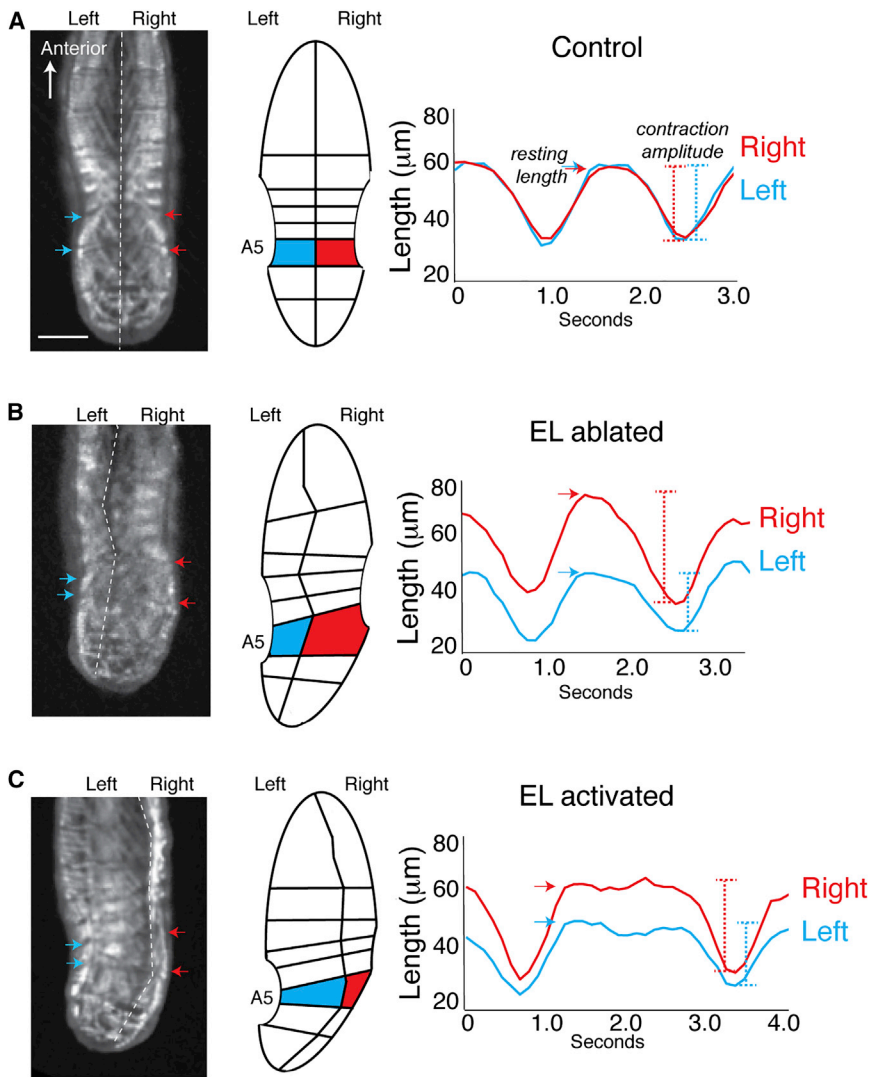
Figure 3. Ablation or Activation of EL Interneurons Results in Failure to Maintain Symmetrical Left-Right Muscle Length without Affecting Left-Right Timing in L1 Larvae

(A–C) Control (A), EL ablated (B), and EL activated (C) larvae quantified for resting muscle length, contraction amplitude, and contraction timing. The left image shows the muscle marker MHC:GFP. The center image shows the schematic of raw data. The right image shows a plot of A5 muscle length on the left (blue) or right (red) over two cycles of relaxation and contraction. The scale bar represents 100 μm. The genotypes are (A and B) *UAS-dTRPA1, MHC:GFP/ UAS-dTRPA1* (A; control at 23°C and n = 8) or (B; activated at 30°C and n = 6). (C) *UAS-reaper, UAS-hid/+; MHC:GFP/+; EL-gal4 /+* (n = 9). See Figure S1 and Movies S6, S7, and S8.

5B–5D and Movie S12). We found that a switch in EL activity was correlated with body bending on the side contralateral to the side with high EL activity (100%, n = 3 larvae, ten switches; Figure 5E). The strong correlation between EL activity and subsequent contralateral motor activity (inferred from body bending) is consistent with EL interneuron activation of contralateral motor neurons.

Identification of Individual EL Interneurons by Light and Electron Microscopy

Our behavioral and functional imaging data support the hypothesis that EL interneurons are part of a sensorimotor circuit that regulates muscle contraction amplitude. To characterize the network context in which the ELs operate, we identified their pre and post-synaptic partners using transmission electron microscopy (TEM) reconstructions. We analyzed multiple hemisegments of two different first instar larvae: one a full CNS reconstruction from a 6 hr old larva, and the other a 1.5 segment reconstruction of A2/A3 segments from a 12–24 hr old larva (Ohyama et al., 2015). Because TEM reconstruction of neural circuits is laborious, we identified a smaller subset of functionally important ELs using the split Gal4 approach (Luan et al., 2006). The *R11F02-gal4* line is expressed in a subset of ELs plus other neurons (Heckscher et al., 2014), so we generated *R11F02-gal4^AD* and *EL-gal4^DBD* lines and crossed them together to label only the R11F02[+] EL^{+} coexpressing neurons (hereafter called 11F02 ∩ ELs). This restricted labeling to just five ELs per hemisegment (Figure 6A). Activation of these five neurons produced a phenotype similar to that seen when activating all ELs with *EL-gal4* (Figures 6B and 6C and Movies S13 and S14). We conclude that the 11F02 ∩ ELs are a functionally relevant subset of the full EL interneuron population.

behavior. We expressed both TRPA1 and GCaMP6 in ELs, induced chronic TRPA1 activation, and imaged EL activity in intact, freely crawling larvae. We observed epochs of left-right asymmetric EL activity in every case (n = 5) (Figure 5A). Interestingly, EL interneurons could undergo repeated left-right switches in activity despite chronic TRPA1 activation; in contrast, similar experiments using isolated CNS preparations never showed left-right switching (Figure 4). We propose that left-right activity switching within the intact larvae is due to sensory input.

Next, we asked whether left-right asymmetrical EL interneuron activity is correlated with a specific larval behavior. We repeated the experiment above using a low-power objective to measure the calcium signal within left and right ELs, while simultaneously monitoring body position using intrinsic autofluorescence of the larvae. We focused our analysis on epochs where EL activation switched from high on one side to high on the other. We selected the ten epochs showing the largest switches in left-right EL activity (without attention to the behavioral data) and aligned the traces to the moment EL activity switched sides (Figures
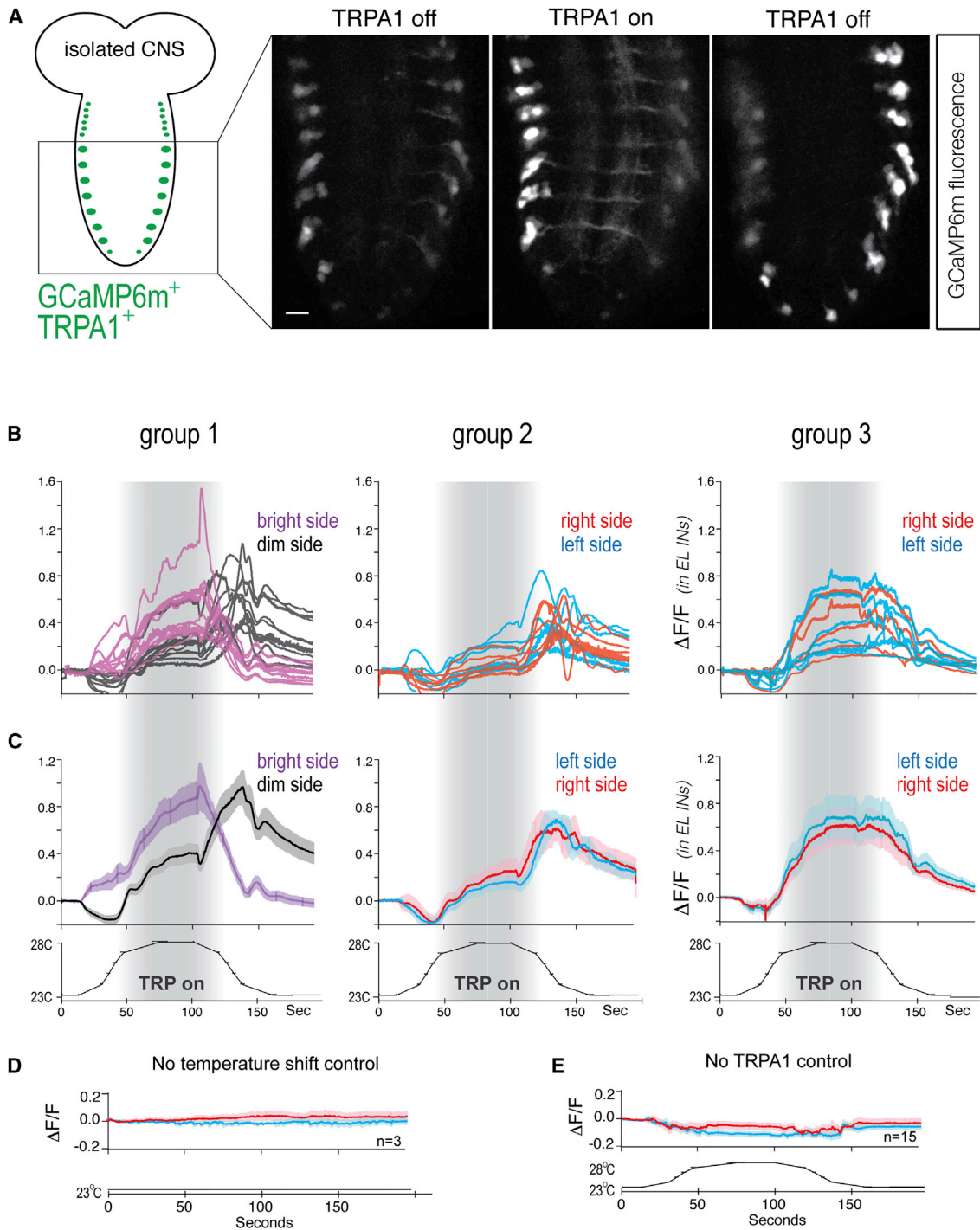
Figure 4. Calcium Imaging Reveals Functional Interactions between Left-Right EL Interneurons

The isolated L1 CNS preparations expressing GCaMP6m and TRPA1 in the ELs. In this experiment, TRPA1 activity cycles from "off" (23°C) to "on" (28°C) and back off (23°C), with the TRPA1 on interval at least 1 min long. There are three classes of response to this experiment (groups 1–3).

(A) The left image shows a schematic of preparation and GCaMP6m/TRPA1 expression in ELs. The right image shows an example from group 1 (Movie S11). Note that both sides start at similar levels, but the left side is more active during the chronic TRPA1 on interval, and the right side becomes more active after TRPA1 stimulus offset. The scale bar represents 25 μm.

(B) Representative individual plots of GCaMP6m fluorescence (ΔF/F) for group 1–group 3.

(legend continued on next page)

To determine the unique morphology of the five 11F02 ∩ EL interneurons, which is a prerequisite for finding the matching neuron in the TEM reconstructions, we used multicolor flip-out (MCFO) (Nern et al., 2015). We found that two ELs had contralateral projections ascending to the brain (A08c and A08s) and three had contralateral projections that remained local (A08e1–A08e3) (Figure 6D). Both projection and local 11F02 ∩ ELs can be distinguished from each other based on their unique 3D pattern of neural arbors (Figure 6D; Table S3). We conclude that each 11F02 ∩ EL interneuron has a distinctive morphology, allowing us to identify the morphologically identical interneurons within the TEM reconstructions.

To identify individual 11F02 ∩ EL interneurons using TEM, we used their shared and distinct features to identify and categorize the neurons (see Experimental Procedures). We use the term "reconstructed" to indicate tracing of all neuronal processes and the term "annotate" for identifying pre and postsynaptic partners. We reconstructed and annotated all five 11F02 ∩ ELs in the younger "Larva 1" TEM volume, which includes the entire CNS (Figures 6E–6I) and the three local 11F02 ∩ ELs in the older "Larva 2" TEM volume, which contains only segment A3 (Figure S3). For each 11F02 ∩ EL interneuron, we observed a stereotyped morphology in multiple segments (Figure 6H), in left and right hemisegments (Figure 6I), and in multiple larvae (Figure S3). No other adjacent neurons in the TEM volumes shared common features with the 11F02 ∩ ELs and matched the MCFO morphology. We conclude that we have identified the 11F02 ∩ EL interneurons in the TEM reconstructions.

The EL Interneurons Receive Direct Proprioceptor Input and Generate Direct Motor Neuron Output

Our first goal was to determine whether the 11F02 ∩ EL interneurons had direct sensory input or direct motor output within the TEM volumes. We benefited from prior annotation of many sensory and motor neurons (Ohyama et al., 2015), but we also reconstructed additional sensory and motor neurons to ensure that each sensory neuron class was represented (chordotonal, external sensory, and proprioceptors) and each motor neuron class was represented (dorsal-, ventral-, and lateral-projecting motor neurons) (Kohsaka et al., 2012; Singhania and Grueber, 2014). We discovered that multiple proprioceptive sensory neurons—but few or no external sensory or chordotonal neurons—formed direct presynaptic contacts with both local and projection EL interneurons (Figures 7A and 7B). The proprioceptors always formed their presynaptic contacts on ipsilateral arbors of the local EL interneurons; that is, left body wall proprioceptors synapse with EL interneurons whose cell bodies are on the left side of the CNS (Figures 7A and 7C). We found that the proprioceptor-EL contacts were highly specific and reproducible across sides of the CNS, multiple segments, and multiple larvae (Figures 7A, S3, and S4). For example, the ventral bipolar dendrite (vbd) proprioceptor always formed presynaptic contacts with the A08e3 arbor, but not the intermingled A08e1 or A08e2 arbors, and the number of vbd contacts was always greater on the A08e3 lateral arbor and fewer on its medial arbor (Figures 7A, 7C, and 7D). The functional significance of different proprioceptors targeting different ELs remains to be determined (see Discussion); however, the specificity and reproducibility of synapse positions and numbers confirm the accuracy of our reconstruction and annotations. The function of proprioceptive neurons in *Drosophila* larvae has not been tested, but proprioceptive neurons monitor muscle length in many insects (Simon and Trimmer, 2009; Tamarkin and Levine, 1996), and thus we propose that the proprioceptor-EL connectivity we observe is used to convey body wall muscle contraction amplitude information to the EL interneurons.

Next, we determined whether EL interneurons formed presynaptic contacts with motor neuron dendrites. We found that the ELs formed direct presynaptic contacts to dorsal-projecting motor neurons RP2, U1, and U2, but not to ventral- or lateral-projecting motor neurons (Figures 7A, 7C, and 7E). The EL interneurons always formed their presynaptic contacts on the contralateral motor neurons; that is, EL interneurons on the left side of the CNS formed presynaptic contacts with motor neurons projecting to the right body wall (Figures 7A and 7C). Thus, if the ELs were to provide excitatory drive to their target motor neurons, it would explain why EL activation correlates with contralateral motor neuron output within intact crawling larvae (see above). Consistent with this hypothesis, we found that ELs are cholinergic (Figure S5), and therefore could provide excitatory drive to motor neurons, similar to previously described cholinergic excitatory premotor neurons (Baines et al., 2001; Pym et al., 2006). Consistent with this conclusion, bilateral Chrimson stimulation of ELs resulted in motor neuron activation (Figure 7F). We conclude that local ELs are functionally presynaptic to contralaterally projecting motor neurons.

Jaam Interneurons: A Link between Proprioceptive Neurons and EL Interneurons

The proprioceptor-EL-motor neuron anatomical circuit described above is unlikely to be functioning in isolation. Thus, we searched for additional neurons that had a similar or greater number of presynaptic contacts with the ELs compared to proprioceptors (see Experimental Procedures). We discovered two interneurons with 8–18 presynaptic contacts per EL interneuron, called Jaam1 and Jaam3 (Figure 8A). Jaam2 had morphology similar to Jaam1/Jaam3, but connected to the ELs via Jaam1 (Figures 8A, inset, and S5). Over 7% of all Jaam1/Jaam3 presynaptic contacts were on the ELs, similar to the combined number of dorsal and ventral proprioceptor neuron inputs to the ELs (Figure 8B, top).

(C) Data from (B) replotted as average plots with SE (genotype: *UAS-dTRPA1/UAS-GCaMP6m; EL-gal4 /EL-gal4*).

(D and E) Controls for isolated CNS preparation experiments.

(D) Preparations expressing GCaMP6m and TRPA1 in ELs held at baseline temperature (23°C) (genotype: *UAS-dTRPA1/UAS-GCaMP6m; EL-gal4 /EL-gal4*).

(E) Preparations expressing only GCaMP6m in ELs with temperature shifts as in (B) and (C) (genotype: *UAS-GCaMP6m/UAS-GCaMP6m; EL-gal4 /EL-gal4*).
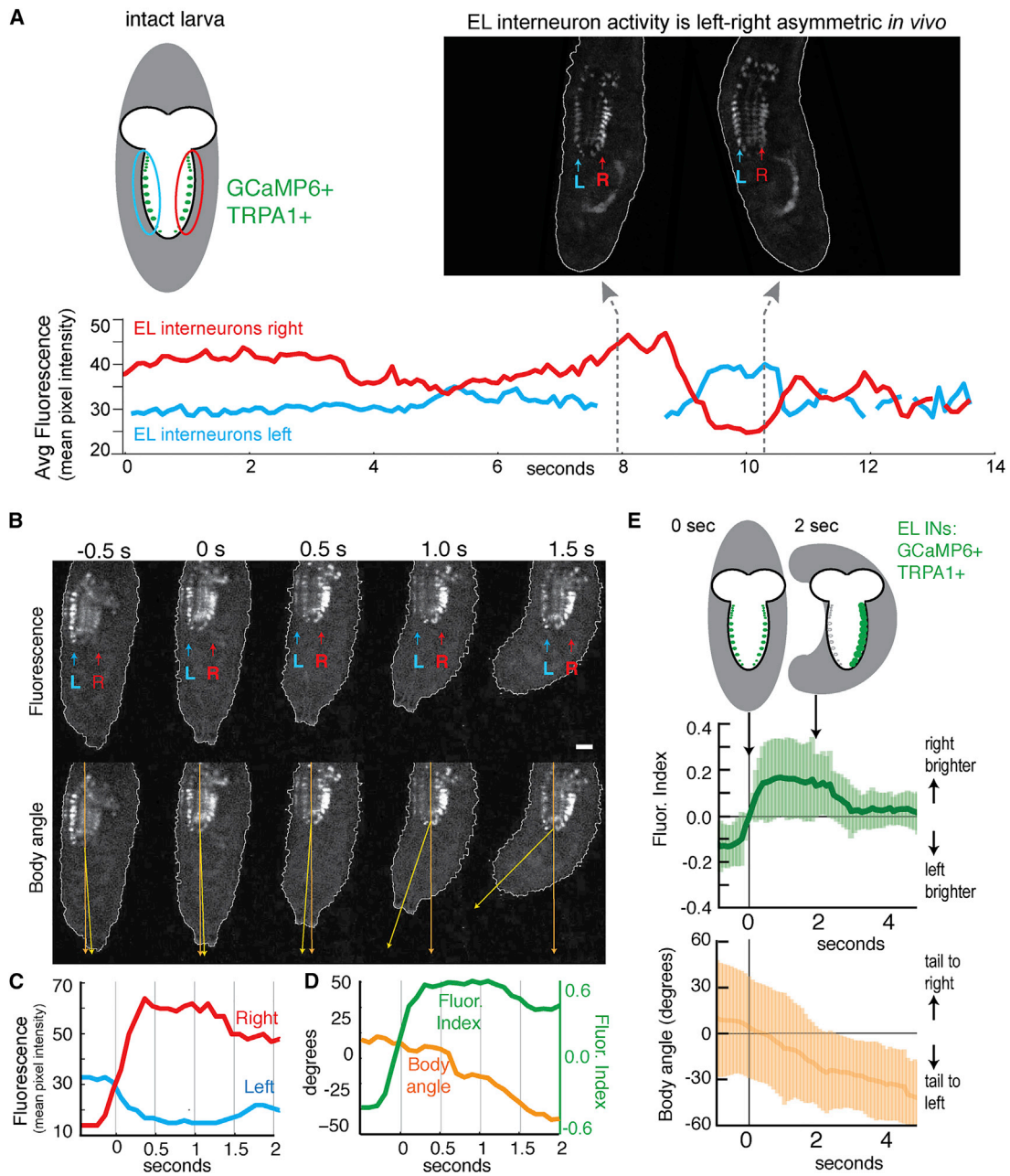
Figure 5. EL Interneuron Activity Is Correlated with Contralateral Muscle Contractions within Freely Crawling Larvae

All data are from intact larvae during forward locomotion with chronic TRPA1 activation of EL interneurons.

(A) The top left image shows a schematic of intact larval preparation and GCaMP6m/TRPA1 expression in EL interneurons. The top right image shows a left-right (L-R) asymmetric GCaMP6m fluorescence in EL interneurons taken from indicated times during plot below (gray arrows). The bottom image shows an intact L1 larvae expressing GCaMP6m and TRPA1 in EL interneurons that were held at 32°C and mean fluorescence intensity was measured in left (blue) and right (red) EL interneurons. Note the blue line is interrupted when fluorescent intensity dropped to levels indistinguishable from background fluorescence (genotype: *UAS-dTRPA1 / UAS-GCaMP6m; EL-gal4 / EL-gal4*).

(B–D) Representative single larva data from Movie S12.

(B) The larva was moving forward, so frames were manually aligned. The top row shows EL GCaMP6m fluorescence (left, L and right, R), and the bottom row shows body angle (arrows). The scale bar represents 50 μm.

(C) Plot of left and right EL fluorescence intensity over the time interval shown in (B).

(D) Plot of fluorescence index (bright side fluorescence, dim side fluorescence / total fluorescence) and body angle for the same time interval shown in (B). The genotype is as in (A).

(E) Averages from ten epochs of left-right EL activity switching in three larvae, aligned to the time of switching (t = 0). The EL activity (green) is correlated with contralateral body bending (orange). The average and SD are shown. The genotype is as in (A).
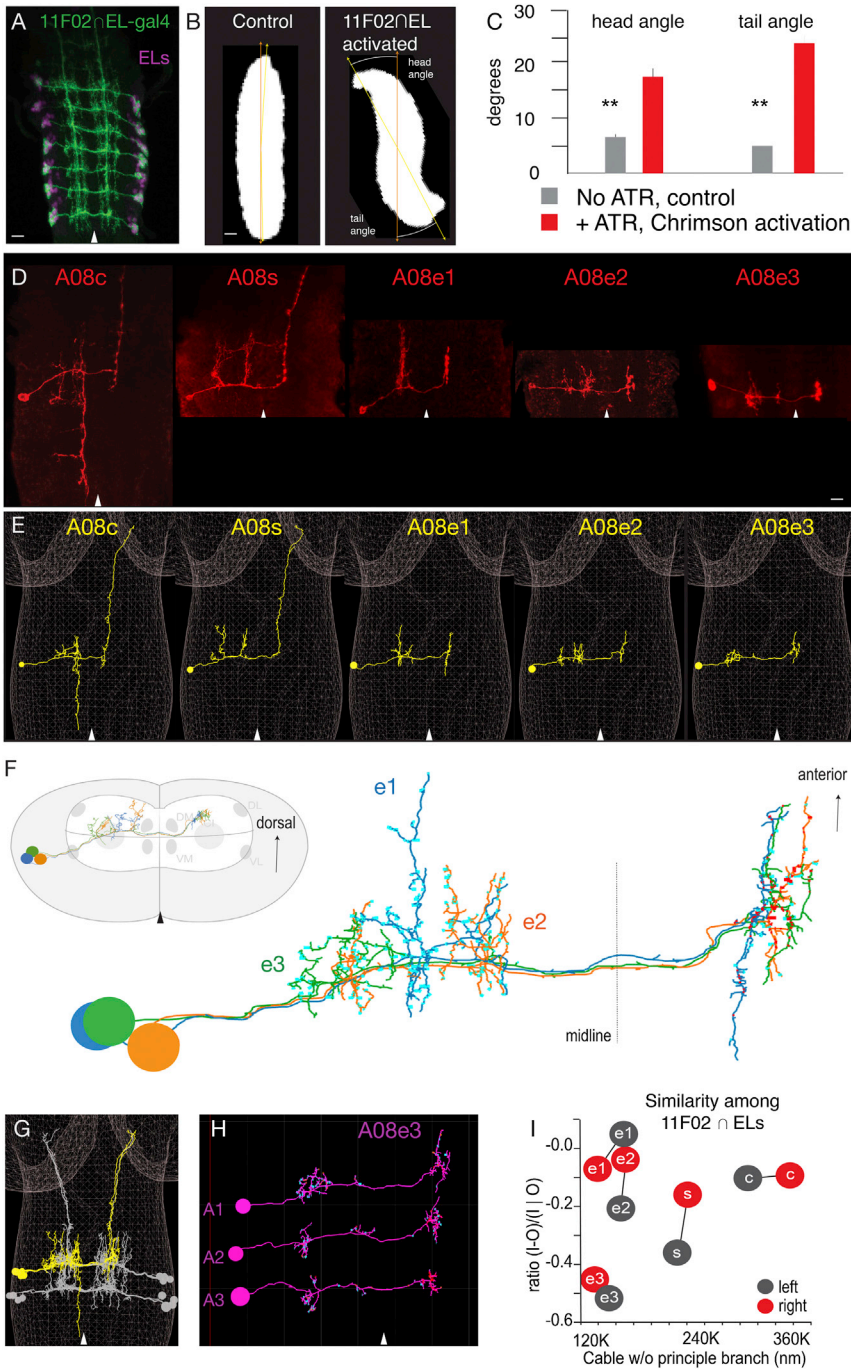
Figure 6. Identification of Individual EL Interneurons by Light and Electron Microscopy

(A–C) Activation of a subset of ELs is sufficient to cause C-bends.

(A) 11F02 ∩ EL-gal4 driving membrane-bound GFP (green) costained for Eve protein (magenta) (anterior up). The scale bar represents 20 μm.

(B and C) Chrimson optogenetic activation of 11F02 ∩ ELs results in larval C-bends. The average and SEM are shown (**p < 0.05 and t test) (genotype: *UAS-Chrimson.mVenus/EL-gal4^{AD}; R11F02-gal4^{DBD}*/+). (Control: larvae raised without ATR and 11F02 ∩ EL activated: raised with ATR). The scale bar represents 100 μm. See Movies S13 and S14.

(D) Individual 11F02 ∩ ELs detected using MCFO. The two projection interneurons (A08c and A08s) and three local interneurons (A08e1–e3) all have contralateral projections (anterior, up and midline, arrowhead). The scale bar represents 5 μm.

(E–H) Individual 11F02 ∩ ELs reconstructed from serial section TEM volume of the younger Larva 1 except where noted (anterior up and midline arrowhead).

(E) Individual 11F02 ∩ ELs are shown below their cognate neurons from MCFO analysis.

(F) A08e1-3 local ELs from the older Larva 2 volume. The upper left image shows a schematic of the posterior/cross section view, with landmark Fasciclin II bundles shown in gray.

(G) All 11F02 ∩ ELs reconstructed in segment A1 and A2; A1L neurons colored yellow. Note the clustered soma and common proximal axon fascicle in the image.

(H) Segmentally homologous neurons are highly similar (A08e3 shown in A1, A2, and A3 left hemisegments).

(I) Bilaterally homologous 11F02 ∩ ELs are more similar to each other than to other ELs (lines show the shortest total path for indicated neurons) (y axis: ratio of input-output/input+output synapse number and x axis: neurite branch length) (total neurite length, principle branch in nm).

arbors (Figures 8A and 8C). In addition, there was specific, reproducible ipsilateral and contralateral connectivity between Jaam1–3 neurons (Figure 8A, inset). Although the functional role of the Jaam neurons in presenting proprioceptive activity to the EL interneurons is currently unknown, it is clear that the Jaam interneurons provide an anatomical link between proprioceptors and EL interneurons.

Saaghi Interneurons: A Link between EL Interneurons and Motor Neurons

We showed above that local EL interneurons formed direct presynaptic contacts with motor neurons. However, the number of synapses between ELs and motor neurons was relatively few (range: 1–7) and were reliably detected with only 3–4 motor
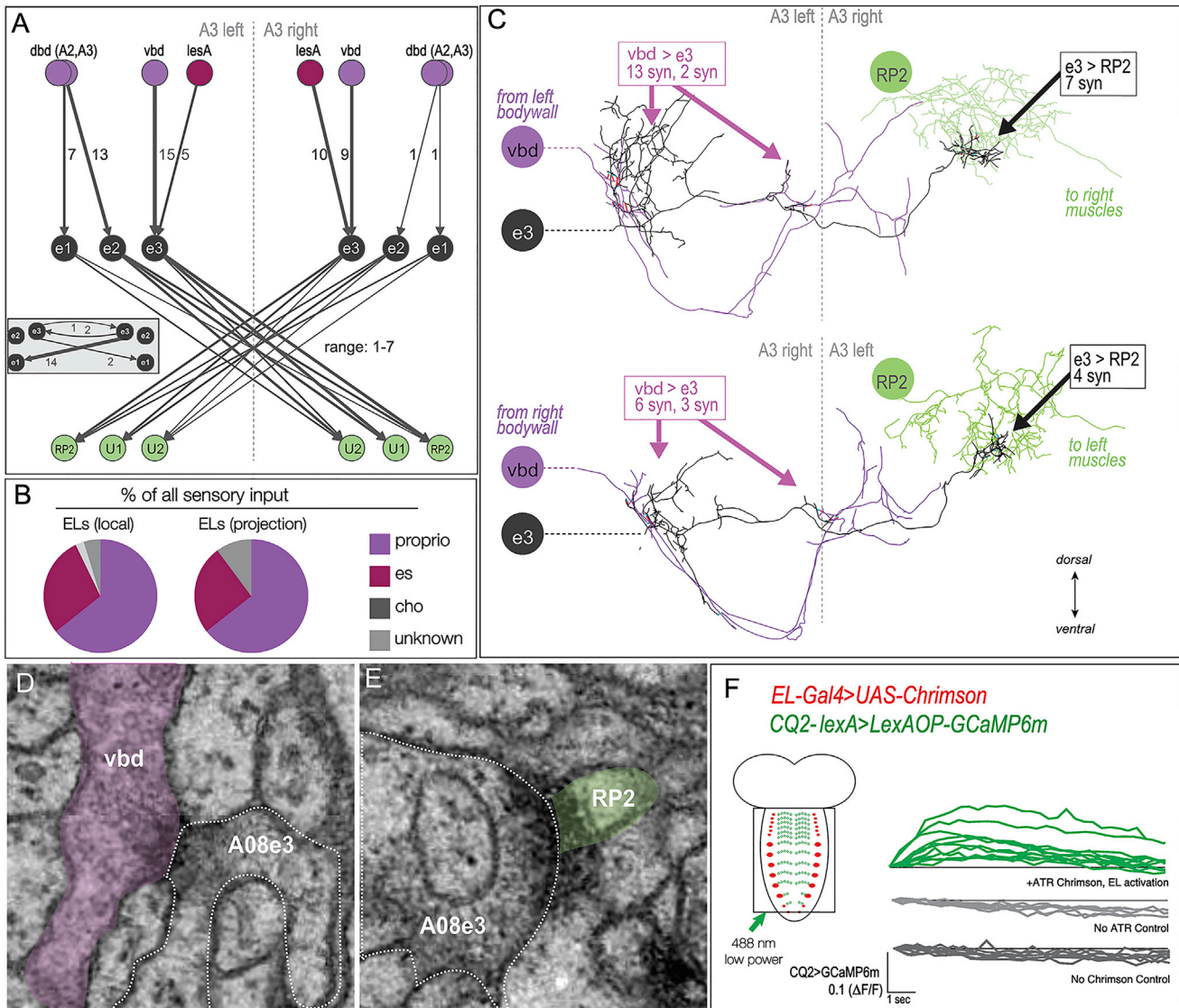
Interestingly, over 30% of the Jaam1–3 neurons inputs were from the dorsal and ventral proprioceptors (Figure 8B, bottom). Thus, the Jaam neurons provide a link from proprioceptors to EL interneurons. Similar to proprioceptor-EL connectivity, Jaam neurons formed highly specific contacts with their input and output neurons. For example, the dorsal bipolar dendrite (dbd) proprioceptive neuron provides input to Jaam1, but not Jaam2/Jaam3, and the Jaam1 neuron provides input to the A08e2, but not A08e1/3, despite their intermingled

Figure 7. Local EL Interneurons Have Monosynaptic Proprioceptive Inputs and Monosynaptic Motor Outputs

An anatomical reconstruction of the sensory-EL-motor neuron pathway in A3 of the older Larva 2.

(A) Summary of the pathway showing the indicated number of synapses between proprioceptive sensory neurons (purple), local ELs (A08e1-A08e3; black), and motor neurons (green). For clarity, the connectivity between local ELs is shown separately (inset). The neurons with unilateral connections were excluded.

(B) Proprioceptive neurons are the sensory class with the most presynaptic contacts on ELs.

(C) The vbd-A08e3-RP2 pathway is bilaterally symmetric at the level of arbor morphology, synapse number, and synapse location. The top image shows the A3 left vbd has two zones of presynaptic contacts with A08e3, which forms synapses with the ventral-most region of the RP2 motor neuron dendritic arbor. The bottom image shows the A3 right vbd-A08e3-RP2 pathway has the similar location and number of synaptic contacts (posterior view, dorsal up and midline, dashed line).

(D and E) Examples of synapse morphology in the TEM reconstruction for vbd-A08e3 (left) and A08e3-RP2 (right). Note the presynaptic vesicle accumulation and electron density at the synapse. The synapses were identified as in Ohyama et al. (2015).

(F) Stimulation of ELs with Chrimson activates dorsal motor neurons. A 488 nm laser illuminated the neuropil, which simultaneously activated Chrimson in ELs (red) and allowed for the visualization of GCaMP6m fluorescence in CQ2-labeled dorsal motor neurons (green). Each line shows the GCaMP6m signal in a different isolated brain preparation. The horizontal lines show baseline fluorescence. The response is significantly different between EL activation and controls (p < 0.05 and chi-square). The top, middle, and bottom data sets are: (top) the indicated genotype + ATR (n = 11); (middle) the indicated genotype without ATR (n = 6); and (bottom) the indicated genotype without UAS-Chrimson and +ATR (n = 7).

neurons of the ~30 per segment. We therefore searched for neurons that had a comparable number of EL presynaptic contacts (see Experimental Procedures). We discovered two interneurons with a range of 2–9 EL presynaptic contacts, which we call Saaghi neurons 1 and 3 (SA1 and SA3; Figures 9A and S6). SA1/SA3 received 10% of all EL presynaptic contacts, far greater than the
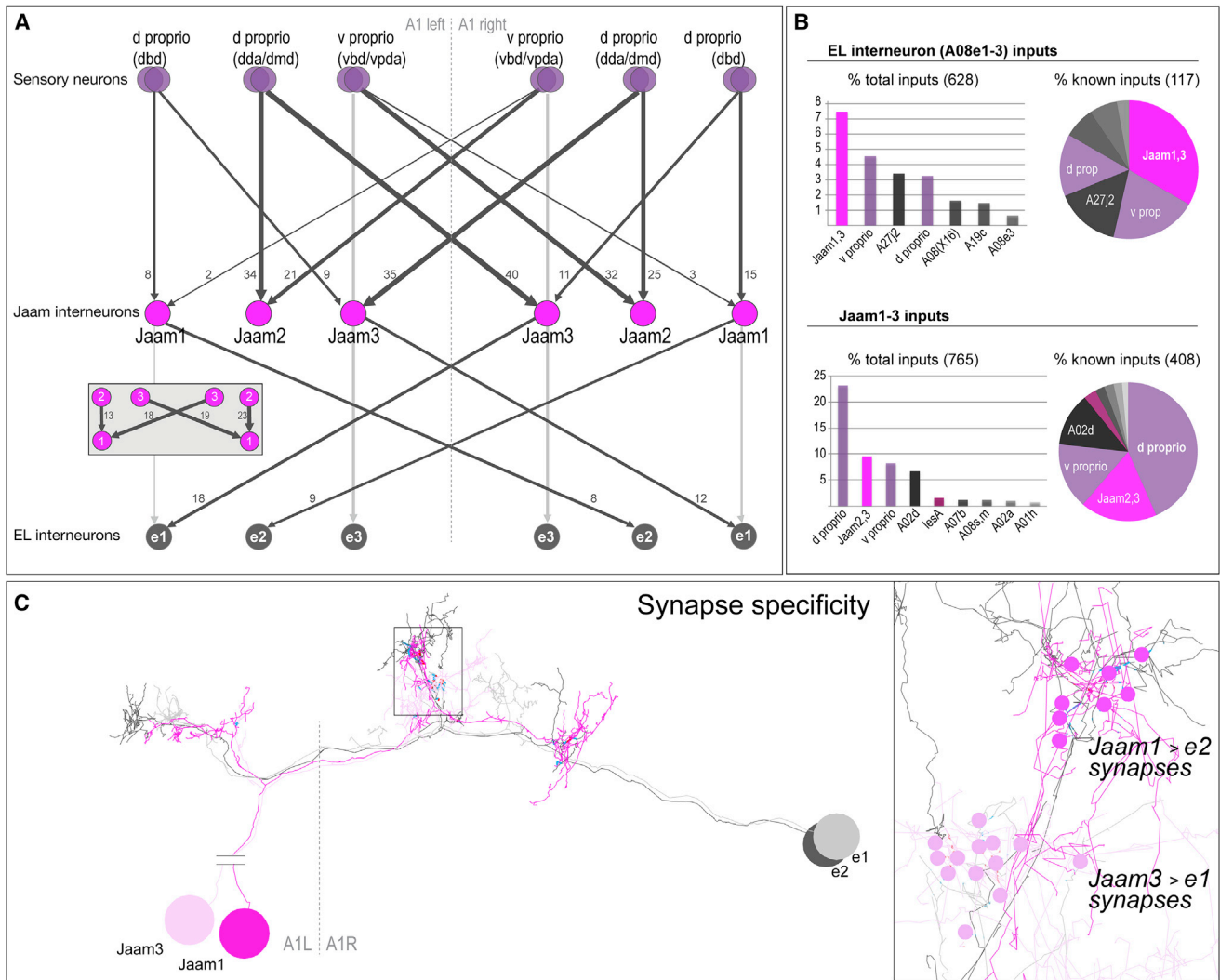
Figure 8. EL Interneurons Have Disynaptic Proprioceptive Inputs

Disynaptic input from proprioceptors to local ELs via the Jaam neurons. The data are from Larva 1, segment A1.

(A) Disynaptic connectivity from proprioceptive sensory neurons (purple) to Jaams (magenta) to local ELs (gray); monosynaptic proprioceptor-EL connectivity shown with light gray lines. For clarity, the connectivity between Jaams is shown separately (inset). The neurons with unilateral connections were excluded.

(B) The top image shows that Jaam1 and 3 neurons provide major inputs into the local EL interneurons (A08e1–e3). The bottom image shows that proprioceptive neurons provide major inputs into the Jaam1–3 neurons. For both the top and bottom, the left graph shows % of total inputs (includes neurons that have not yet been fully reconstructed) and the right graph shows % of known inputs (only fully reconstructed and annotated neurons).

(C) Synaptic specificity: Jaam1 (dark magenta) and Jaam3 (light magenta) reproducibly target distinct, stereotyped regions of the different EL interneuronal arbors (light gray, A08e1 and dark gray, A08e2), as seen in the inset (right) (posterior view, dorsal up and midline, dashed line).

number of EL presynaptic contacts to dorsal-projecting motor neurons (Figure 9B, top). In contrast to the EL interneurons, which had outputs to only the dorsal-projecting motor neurons, the SA1/SA3 neurons had outputs to all classes of motor neurons (Figure 9A). For example, SA1 formed over 33–37 presynaptic contacts with dorsal-projecting motor neurons, 15–33 to ventral-projecting motor neurons, and 2–8 to lateral-projecting motor neurons (Figure 9A). Moreover, the SA1/SA3 neurons allocated 20% of their total presynaptic contacts to motor neurons (Figure 9B, bottom). Thus, the SA1/SA3 premotor neurons provide a link from EL interneurons to all classes of motor neurons.

Interestingly, the disynaptic EL-SA-motor neuron pathway connects the ELs with ipsilateral motor neurons (Figure 9A, black lines), whereas the monosynaptic EL-motor neuron pathway connects ELs to contralateral motor neurons (Figure 9A, gray lines). These two pathways could generate synergistic output if the SA neurons are inhibitory (see Discussion).

In contrast to the specificity of proprioceptor-EL connectivity, the EL-SA-motor neuron connectivity is distributed; each EL interneuron synapses with both SA neurons, and each SA neuron synapses with all motor neuron classes (Figure 9C). This shows that the EL interneurons have the potential to regulate the activity
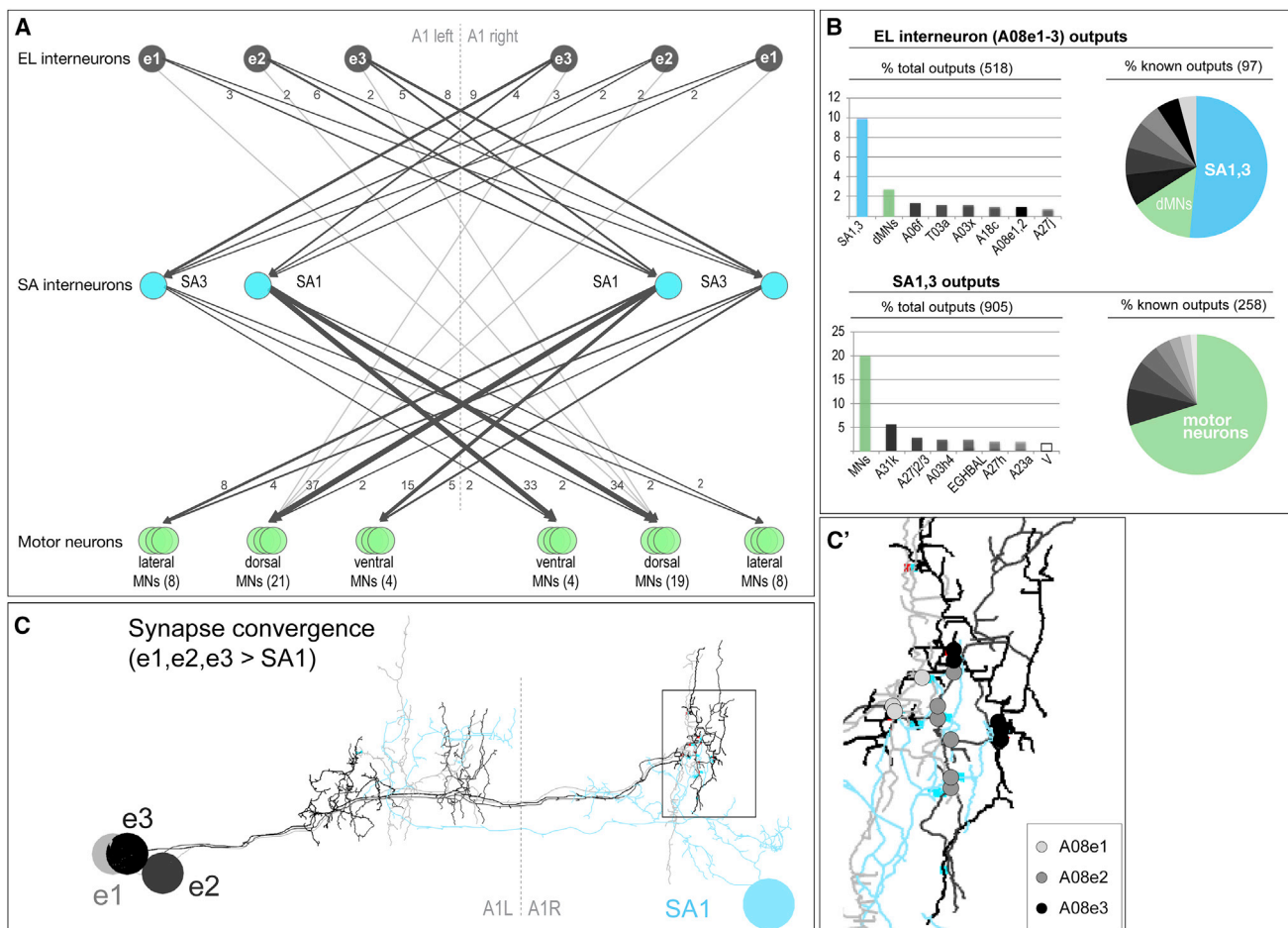
Figure 9. EL Interneurons Have Disynaptic Motor Neuron Outputs

Anatomical circuit reconstruction of EL-SA-motor neuron pathway from Larva 1 segment A1 reveals the 11F02 ∩ ELs have disynaptic motor neuron output via the SA interneurons.

(A) Synaptic connections between local ELs (gray), premotor SAs (cyan), and motor neurons (green). The monosynaptic EL-MN connectivity is shown with light gray lines. Only the bilateral connections between specific neurons (ELs and SAs) or motor neuron groups (dorsal, ventral, and lateral) are shown. The number of motor neurons in each class is shown in parentheses.

(B) The top image shows the major output of the 11F02 ∩ ELs are the SAs. The bottom image shows the major output of the SAs are motor neurons.

(C) The three local ELs A08e1–e3 (from light to dark gray) project to a common region of the SA1 dendritic arbor; (C') enlargement of boxed region in (C) (posterior view, dorsal up and midline, dashed line).

of all body wall muscles and suggests that different mechanisms of circuit formation may be used by proprioceptor-Jaam-ELs and by EL-SA-motor neurons. Although the role of the SA1/SA3 neurons in translating EL activity into motor output is currently unknown, our data show EL interneurons are positioned at the heart of an anatomical sensorimotor circuit that is well suited for detecting and modifying body wall muscle contraction and body posture.

DISCUSSION

Drosophila Larvae: A Model System for Investigating Left-Right Symmetric Motor Output

Bilaterally symmetric motor patterns—those with muscle contractions on the left and right sides of the body occurring synchronously and with equal amplitude—have broad and essential functions. Despite the nearly ubiquitous use of bilaterally symmetric motor patterns throughout the animal kingdom, we understand surprisingly little about the relevant neural circuitry. Here, we identify an anatomical sensorimotor circuit containing an evolutionarily conserved population of Eve/Evx⁺ interneurons that is required to maintain left-right symmetric muscle contraction amplitude both during active muscle contraction and at rest. To our knowledge, these interneurons are the first known to regulate bilaterally symmetric muscle contraction amplitude. In mouse, Sim1⁺ V3 interneurons have a related function during alternating gait (Zhang et al., 2008). In the future, it will be interesting to directly examine muscle contraction amplitude in "V3 defective" mice to determine whether this class of interneuron is responsible for balancing amplitude of left-right muscle

contraction during alternating motor patterns. Similarly, it will be interesting to determine the role of *Drosophila* Single-minded (Sim)[+] interneurons during left-right symmetric motor output.

EL Interneurons Are Part of a Sensorimotor Circuit

We show that EL interneurons act in a sensorimotor circuit independent of the CPG that generates locomotion. First, in the absence of sensory input, ELs do not show locomotion-like patterns of activity (Figure S2). Second, EL perturbation does not alter left-right timing of muscle contraction (Figure 3). Third, EL perturbation alters muscle contraction amplitude during locomotion and at rest (Figure 3).

Our data suggest that EL interneurons receive sensory input that is primarily proprioceptive. Because proprioceptive neurons can detect muscle length and movement (Simon and Trimmer, 2009; Tamarkin and Levine, 1996), they are well suited to convey muscle amplitude information to the ELs. Closer inspection of the proprioceptor to EL connectivity generates interesting hypotheses. First, proprioceptors are presynaptic to both projection and local EL interneurons; the former may send body posture information to the brain, while the latter may act locally to maintain left-right symmetric muscle length in each segment. Second, the Jaam interneurons are well positioned to process sensory information (e.g., from dorsal or ventral regions of the body wall) prior to transmitting information to the ELs. Although we currently know little about Jaam neurotransmitter expression or function, their position in the circuit raises the question of whether EL interneurons show state-dependent responses to proprioceptive inputs.

Our data demonstrate that EL interneurons are presynaptic to motor neurons and can modify motor output. EL perturbation results in slow crawling and asymmetric left-right muscle contraction amplitude, while optogenetic stimulation of ELs induces motor neuron activity. The majority of ELs are cholinergic and likely excitatory, they provide direct input to contralateral motor neurons, and motor neurons are glutamatergic and excitatory (Kohsaka et al., 2012). Thus, EL activity on one side of the body should result in increased contralateral motor neuron activity and contralateral muscle contraction. This may be reinforced by the disynaptic (EL-SA-MN) pathway, in which EL activity would prevent ipsilateral motor neuron activity if the SA neurons were inhibitory. This model awaits future characterization of SA neurotransmitter expression and function. We propose the hypothesis that ipsilateral muscle relaxation (via the EL-SA-MN pathway) and contralateral muscle contraction (via the direct EL-MN pathway) are used for dynamic adjustment of body posture.

How Do EL Interneurons Maintain Left-Right Symmetric Muscle Contraction Amplitude?

Left-right differences in muscle contraction amplitude inevitably arise due to stochastic external (environmental) or internal (CNS/muscle) asymmetries. Without proper compensation, these perturbations would result in mismatched muscle contraction amplitude on left-right sides of the body. We hypothesize that sensory input generates a representation of body wall curvature that is delivered to the EL interneurons. Left-right interactions among ELs would allow them to compare left versus the right sides of the body, followed by EL stimulation of motor output to restore left-right symmetric muscle length.

How does EL interneuron ablation and activation generate the same phenotype? We favor a model in which ELs are part of a "perturbation-compensation" circuit. A larva that experiences an asymmetrical perturbation from an external or internal source would generate left-right mismatched muscle contraction amplitudes in the absence of any compensation. We propose that the EL circuit detects and compensates for these asymmetries. When the ELs are absent or constitutively active, they lose the ability to perform the left-right comparison and the asymmetries persist. In this way, two "opposite" manipulations yield the "same" phenotype.

A Conserved Function of Eve/Evx[+] Interneurons in Neuronal Circuitry and Behavior?

There is deep conservation of genetic programs that specify neuronal fate. This is particularly true for the Eve/Evx[+] interneurons, which have been found in all bilateral animals examined to date except *C. elegans*. Annelids, chordates, insects, fish, birds, and mammals—as well as the presumed last common ancestor between invertebrates and vertebrates, *Platynereis dumerilii*—all contain Eve/Evx[+] interneurons (Avaron et al., 2003; Copf et al., 2003; Denes et al., 2007; Ferrier et al., 2001; Fujioka et al., 2003; Holland, 2013; Ikuta et al., 2004; Landgraf et al., 1999; Moran-Rivard et al., 2001; Sordino et al., 1996; Suster et al., 2009; Takatori et al., 2008; Thaëron et al., 2000). Evx^{+} neurons in mice are commissural, excitatory, and directly contact motor neurons (Lanuza et al., 2004; Moran-Rivard et al., 2001); here, we show that fly Eve[+] interneurons are commissural, likely excitatory, and directly contact motor neurons. A hypothesis to explain the remarkable parallels between Eve/Evx[+] interneurons is that the last common ancestor between vertebrates and invertebrates was segmented and motile; and thus the genetic programs used to create locomotor circuitry may be evolutionarily ancient.

We have shown that the *Drosophila* Eve[+] lateral interneurons are required to maintain left-right symmetrical motor output in the larva. Do Evx[+] interneurons have a similar function in other organisms? Genetic removal of Evx1^{+} interneurons in mice did not reveal any specific function in either gross motor patterns or in the timing of left-right alternating motor neuronal activity as assayed by nerve root recordings (Lanuza et al., 2004; Moran-Rivard et al., 2001). Subsequently, a broader genetic manipulation which reduced the number of Evx1^{+} interneurons to 25% of wild-type levels, as well as ablating a large, but unspecified number of Evx1^{−} neurons, resulted in a hind limb hopping phenotype during fast locomotion (Talpalar et al., 2013). This study raised the possibility that Evx1^{+} interneurons regulate locomotion in mice. In our study, we show that highly specific ablation or activation of Eve[+] lateral interneurons disrupts larval crawling. It will be interesting to determine whether Evx1^{+} interneurons regulate bilaterally symmetric or alternating gait in other organisms, as well as whether Eve[+] interneurons regulate alternating gait or symmetric flight in adult flies.

EXPERIMENTAL PROCEDURES

Fly Genetics

For a complete list of fly stocks see Supplemental Information. For *EL-AD* and *CQ2-lexA*, molecular constructs and transgenic flies were generated

using standard methods as previously described (Pfeiffer et al., 2008, 2010).

Embryo Immunostaining

We used standard methods to stain *Drosophila* embryos and larvae (Manning et al., 2012). For a list of primary antibodies see Supplemental Information. Secondary antibodies were from Invitrogen/Molecular Probes and were used according to manufacturer's instructions. Images were acquired on a Zeiss 700 or 710 confocal microscope with a 40× objective. Images were cropped in ImageJ (NIH) and assembled in Illustrator and Photoshop (Adobe).

Larval Behavior

We recorded behavior in newly hatched larvae (0–4 hr old), except Chrimson experiments were done in late first instar to second larvae.

Brightfield Whole Larval Recordings

Behavior arenas were made of 6% agar in grape or apple juice, 2 mm thick. Behavior was recorded at 23°C, unless otherwise noted. The temperature was measured using an Omega HH508 thermometer and controlled with a custom-built thermoelectric controller and peltier device. The arenas were placed under a Leica S8APO dissecting microscope and a red light (700 nm, Metaphase Technologies) illuminated a single larva. The microscope was equipped with a Scion 1394 Camera, using Scion VisiCapture software. Images were acquired at either 4 Hz or 7.5 Hz. All larvae were fed yeast paste lacking all-trans-retinal (ATR) except where noted. Also see Supplemental Information.

Fluorescent Whole Larval Recordings, Muscle Kinematics

Behavior arenas were placed on sapphire slides. Larva were allowed to cross the field of view then the stage was manually moved to keep the larvae in view, resulting in several recordings per larva. Images were acquired at 10 Hz with a 10× objective on a McBain spinning disc confocal microscope equipped with a Hamamatsu EM-CCD camera, and Volocity software (PerkinElmer). For image analysis see Supplemental Information.

Calcium Imaging

For Figure 4, a freshly dissected CNS from a newly hatched larva was placed directly on sapphire slides in HL3.1 saline. Note there were fine manual adjustments for small changes in focal plane upon temperature shift. For Figure 5 intact larval recordings, see "Fluorescent whole larval recordings, muscle kinematics" section above. The relationship between the EL calcium signal and body position was complex, so we focused our analysis on epochs where EL activation switched from high on one side to high on the other. For Figure 7C, a freshly dissected CNS from a newly hatched larva was placed on a slide in HL3.1 saline. A region of interest encompassing the nerve cord neuropil, with motor neuron dendrites in focus, was illuminated with 488 nm light at 10% laser power to simultaneously activate Chrimson and monitor GCaMP6m fluorescence. For Figure S2, we used the protocol as described above, except we used Baines' saline (Marley and Baines, 2011) and maintained a constant temperature between 26°C–28°C. Temperature was controlled as described above. Imaging was done with a 40× objective on the McBain spinning disc, as described above. For details of image analysis see Supplemental Information.

MCFO to Label and Name Single EL Interneurons

We used published methods to label single EL interneurons in first instar larvae (Nern et al., 2015). The stock *MCFO-3* was crossed to *EL-gal4* (Supplemental Information). The progeny first instar larvae were dissected, stained for the MCFO epitopes and Eve protein, and imaged on a Zeiss 700 or 710 confocal microscope. Segments containing single MCFO$^+$ Eve$^+$ neurons were analyzed in dorsal view and posterior view, which allowed each neuron to be classified as one of the five 11F02 ∩ ELs. The name of each 11F02 ∩ EL interneuron was chosen to match its name in the third instar abdominal CNS. Jaam is Persian for "wineglass" (reflecting the strong association with sensory input) and saaghi (SA neurons) is Persian for "one who brings a gift" (reflecting their role in presenting information to the motor neurons).

Reconstructing Single EL Interneurons and Determining Their Synaptic Partners within the Serial Section TEM Volumes

We used two larval reconstructions: one a full CNS reconstruction from a 6 hr old first instar larva, and the other a 1.5 segment reconstruction of A2/A3 seg-ments from a 12–24 hr old first instar larva (Ohyama et al., 2015). We recon-structed neurons in CATMAID using a Google Chrome browser as previously described (Ohyama et al., 2015). To identify single EL interneurons within the TEM volume, we used the following features observed in the MCFO "ground truth" data set: (1) All 11F02 ∩ ELs share a common ventro-anterior cell body position; (2) all 11F02 ∩ ELs share a common proximal axon fascicle; (3) all 11F02 ∩ ELs have contralateral projections; and (4) each 11F02 ∩ ELs has a characteristic morphology when viewed dorsally and posteriorly (Table S3). Using these criteria, we reconstructed neurons with ventro-anterior soma until we found one that matched the morphology of an individual 11F02 ∩ EL inter-neuron; we then reconstructed adjacent neurons projecting in a common proximal axon fascicle to "enrich" for the remaining 11F02 ∩ ELs. Note, only bilaterally symmetric connections are shown in Figures 7, 8, and 9.

To identify direct sensory inputs and motor outputs, we relied on previously reconstructed sensory and motor neurons, supplemented by reconstruction of under-represented classes such as lateral projecting motor neurons and proprioceptive sensory neurons. To identify interneurons with direct pre-synaptic connections to EL interneurons, we reconstructed neurites that con-tacted clusters of post-synaptic sites on EL arbors. If a reconstructed neuron accumulated several (3+) presynaptic contacts with an EL interneuron, we continued reconstruction. In this way, we could rapidly focus on the neurons with the greatest number of presynaptic contacts with an EL interneuron. Similar methods were used to identify neurons post-synaptic to each EL interneuron.

SUPPLEMENTAL INFORMATION

Supplemental Information includes Supplemental Experimental Procedures, seven figures, three tables, and 14 movies and can be found with this article online at http://dx.doi.org/10.1016/j.neuron.2015.09.009.

REFERENCES

Avaron, F., Thaëron-Antono, C., Beck, C.W., Borday-Birraux, V., Géraudie, J., Casane, D., and Laurenti, P. (2003). Comparison of even-skipped related gene expression pattern in vertebrates shows an association between expression domain loss and modification of selective constraints on sequences. Evol. Dev. *5*, 145–156.

Baines, R.A., Uhler, J.P., Thompson, A., Sweeney, S.T., and Bate, M. (2001). Altered electrical properties in Drosophila neurons developing without synaptic transmission. J. Neurosci. *21*, 1523–1531.

Berni, J. (2015). Genetic dissection of a regionally differentiated network for exploratory behavior in Drosophila larvae. Curr. Biol. *25*, 1319–1326.

Berni, J., Pulver, S.R., Griffith, L.C., and Bate, M. (2012). Autonomous circuitry for substrate exploration in freely moving Drosophila larvae. Curr. Biol. *22*, 1861–1870.

Bouvier, J., Thoby-Brisson, M., Renier, N., Dubreuil, V., Ericson, J., Champagnat, J., Pierani, A., Chédotal, A., and Fortin, G. (2010). Hindbrain interneurons and axon guidance signaling critical for breathing. Nat. Neurosci. *13*, 1066–1074.

Broihier, H.T., and Skeath, J.B. (2002). Drosophila homeodomain protein dHb9 directs neuronal fate via crossrepressive and cell-nonautonomous mechanisms. Neuron *35*, 39–50.

Clyne, J.D., and Miesenböck, G. (2008). Sex-specific control and tuning of the pattern generator for courtship song in Drosophila. Cell *133*, 354–363.

Copf, T., Rabet, N., Celniker, S.E., and Averof, M. (2003). Posterior patterning genes and the identification of a unique body region in the brine shrimp Artemia franciscana. Development *130*, 5915–5927.

Crisp, S., Evers, J.F., Fiala, A., and Bate, M. (2008). The development of motor coordination in Drosophila embryos. Development *135*, 3707–3717.

Crisp, S.J., Evers, J.F., and Bate, M. (2011). Endogenous patterns of activity are required for the maturation of a motor network. J. Neurosci. *31*, 10445–10450.

Denes, A.S., Jékely, G., Steinmetz, P.R., Raible, F., Snyman, H., Prud'homme, B., Ferrier, D.E., Balavoine, G., and Arendt, D. (2007). Molecular architecture of annelid nerve cord supports common origin of nervous system centralization in bilateria. Cell *129*, 277–288.

Dixit, R., Vijayraghavan, K., and Bate, M. (2008). Hox genes and the regulation of movement in Drosophila. Dev. Neurobiol. *68*, 309–316.

Doe, C.Q., Smouse, D., and Goodman, C.S. (1988). Control of neuronal fate by the Drosophila segmentation gene even-skipped. Nature *333*, 376–378.

Dubayle, D., and Viala, D. (1996). Localization of the spinal respiratory rhythm generator by an in vitro electrophysiological approach. Neuroreport *7*, 1175–1180.

Esmaeili, B., Ross, J.M., Neades, C., Miller, D.M., 3rd, and Ahringer, J. (2002). The C. elegans even-skipped homologue, vab-7, specifies DB motoneurone identity and axon trajectory. Development *129*, 853–862.

Ferrier, D.E., Minguillón, C., Cebrián, C., and Garcia-Fernàndez, J. (2001). Amphioxus Evx genes: implications for the evolution of the Midbrain-Hindbrain Boundary and the chordate tailbud. Dev. Biol. *237*, 270–281.

Frasch, M., Hoey, T., Rushlow, C., Doyle, H., and Levine, M. (1987). Characterization and localization of the even-skipped protein of Drosophila. EMBO J. *6*, 749–759.

Fujioka, M., Emi-Sarker, Y., Yusibova, G.L., Goto, T., and Jaynes, J.B. (1999). Analysis of an even-skipped rescue transgene reveals both composite and discrete neuronal and early blastoderm enhancers, and multi-stripe positioning by gap gene repressor gradients. Development *126*, 2527–2538.

Fujioka, M., Lear, B.C., Landgraf, M., Yusibova, G.L., Zhou, J., Riley, K.M., Patel, N.H., and Jaynes, J.B. (2003). Even-skipped, acting as a repressor, regulates axonal projections in Drosophila. Development *130*, 5385–5400.

Heckscher, E.S., Lockery, S.R., and Doe, C.Q. (2012). Characterization of Drosophila larval crawling at the level of organism, segment, and somatic body wall musculature. J. Neurosci. *32*, 12460–12471.

Heckscher, E.S., Long, F., Layden, M.J., Chuang, C.H., Manning, L., Richart, J., Pearson, J.C., Crews, S.T., Peng, H., Myers, E., and Doe, C.Q. (2014). Atlas-builder software and the eNeuro atlas: resources for developmental biology and neuroscience. Development *141*, 2524–2532.

Holland, P.W. (2013). Evolution of homeobox genes. Wiley Interdiscip. Rev. Dev. Biol. *2*, 31–45.

Hughes, C.L., and Thomas, J.B. (2007). A sensory feedback circuit coordinates muscle activity in Drosophila. Mol. Cell. Neurosci. *35*, 383–396.

Ikuta, T., Yoshida, N., Satoh, N., and Saiga, H. (2004). Ciona intestinalis Hox gene cluster: Its dispersed structure and residual colinear expression in development. Proc. Natl. Acad. Sci. USA *101*, 15118–15123.

Jahan-Parwar, B., and Fredman, S.M. (1980). Motor program for pedal waves during Aplysia locomotion is generated in the pedal ganglia. Brain Res. Bull. *5*, 169–177.

Kohsaka, H., Okusawa, S., Itakura, Y., Fushiki, A., and Nose, A. (2012). Development of larval motor circuits in Drosophila. Dev. Growth Differ. *54*, 408–419.

Kohsaka, H., Takasu, E., Morimoto, T., and Nose, A. (2014). A group of segmental premotor interneurons regulates the speed of axial locomotion in Drosophila larvae. Curr. Biol. *24*, 2632–2642.

Lahiri, S., Shen, K., Klein, M., Tang, A., Kane, E., Gershow, M., Garrity, P., and Samuel, A.D. (2011). Two alternating motor programs drive navigation in Drosophila larva. PLoS ONE *6*, e23180.

Landgraf, M., Roy, S., Prokop, A., VijayRaghavan, K., and Bate, M. (1999). Even-skipped determines the dorsal growth of motor axons in Drosophila. Neuron *22*, 43–52.

Lanuza, G.M., Gosgnach, S., Pierani, A., Jessell, T.M., and Goulding, M. (2004). Genetic identification of spinal interneurons that coordinate left-right locomotor activity necessary for walking movements. Neuron *42*, 375–386.

Luan, H., Peabody, N.C., Vinson, C.R., and White, B.H. (2006). Refined spatial manipulation of neuronal function by combinatorial restriction of transgene expression. Neuron *52*, 425–436.

Manning, L., Heckscher, E.S., Purice, M.D., Roberts, J., Bennett, A.L., Kroll, J.R., Pollard, J.L., Strader, M.E., Lupton, J.R., Dyukareva, A.V., et al. (2012). A resource for manipulating gene expression and analyzing cis-regulatory modules in the Drosophila CNS. Cell Rep. *2*, 1002–1013.

Marley, R., and Baines, R.A. (2011). Dissection of first- and second-instar Drosophila larvae for electrophysiological recording from neurons: the flat (or fillet) preparation. Cold Spring Harb. Protoc. *2011*, 2011.

Moran-Rivard, L., Kagawa, T., Saueressig, H., Gross, M.K., Burrill, J., and Goulding, M. (2001). Evx1 is a postmitotic determinant of v0 interneuron identity in the spinal cord. Neuron *29*, 385–399.

Murchison, D., Chrachri, A., and Mulloney, B. (1993). A separate local pattern-generating circuit controls the movements of each swimmeret in crayfish. J. Neurophysiol. *70*, 2620–2631.

Nern, A., Pfeiffer, B.D., and Rubin, G.M. (2015). Optimized tools for multicolor stochastic labeling reveal diverse stereotyped cell arrangements in the fly visual system. Proc. Natl. Acad. Sci. USA *112*, E2967–E2976.

Ohyama, T., Schneider-Mizell, C.M., Fetter, R.D., Aleman, J.V., Franconville, R., Rivera-Alba, M., Mensh, B.D., Branson, K.M., Simpson, J.H., Truman, J.W., et al. (2015). A multilevel multimodal circuit enhances action selection in Drosophila. Nature *520*, 633–639.

Pfeiffer, B.D., Jenett, A., Hammonds, A.S., Ngo, T.T., Misra, S., Murphy, C., Scully, A., Carlson, J.W., Wan, K.H., Laverty, T.R., et al. (2008). Tools for neuroanatomy and neurogenetics in Drosophila. Proc. Natl. Acad. Sci. USA *105*, 9715–9720.

Pfeiffer, B.D., Ngo, T.T., Hibbard, K.L., Murphy, C., Jenett, A., Truman, J.W., and Rubin, G.M. (2010). Refinement of tools for targeted gene expression in Drosophila. Genetics *186*, 735–755.

Pulver, S.R., and Griffith, L.C. (2010). Spike integration and cellular memory in a rhythmic network from Na+/K+ pump current dynamics. Nat. Neurosci. *13*, 53–59.

Pulver, S.R., Pashkovski, S.L., Hornstein, N.J., Garrity, P.A., and Griffith, L.C. (2009). Temporal dynamics of neuronal activation by Channelrhodopsin-2 and TRPA1 determine behavioral output in Drosophila larvae. J. Neurophysiol. *101*, 3075–3088.

Pym, E.C., Southall, T.D., Mee, C.J., Brand, A.H., and Baines, R.A. (2006). The homeobox transcription factor Even-skipped regulates acquisition of electrical properties in Drosophila neurons. Neural Dev. *1*, 3.

Rickert, C., Kunz, T., Harris, K.L., Whitington, P.M., and Technau, G.M. (2011). Morphological characterization of the entire interneuron population reveals principles of neuromere organization in the ventral nerve cord of Drosophila. J. Neurosci. *31*, 15870–15883.

Schaefer, J.E., Worrell, J.W., and Levine, R.B. (2010). Role of intrinsic properties in Drosophila motoneuron recruitment during fictive crawling. J. Neurophysiol. *104*, 1257–1266.

Simon, M.A., and Trimmer, B.A. (2009). Movement encoding by a stretch receptor in the soft-bodied caterpillar, Manduca sexta. J. Exp. Biol. *212*, 1021–1031.

Singhania, A., and Grueber, W.B. (2014). Development of the embryonic and larval peripheral nervous system of Drosophila. Wiley Interdiscip. Rev. Dev. Biol. *3*, 193–210.

Sordino, P., Duboule, D., and Kondo, T. (1996). Zebrafish Hoxa and Evx-2 genes: cloning, developmental expression and implications for the functional evolution of posterior Hox genes. Mech. Dev. *59*, 165–175.

Suster, M.L., Kania, A., Liao, M., Asakawa, K., Charron, F., Kawakami, K., and Drapeau, P. (2009). A novel conserved evx1 enhancer links spinal interneuron morphology and cis-regulation from fish to mammals. Dev. Biol. *325*, 422–433.

Takatori, N., Butts, T., Candiani, S., Pestarino, M., Ferrier, D.E., Saiga, H., and Holland, P.W. (2008). Comprehensive survey and classification of homeobox genes in the genome of amphioxus, Branchiostoma floridae. Dev. Genes Evol. *218*, 579–590.

Talpalar, A.E., Bouvier, J., Borgius, L., Fortin, G., Pierani, A., and Kiehn, O. (2013). Dual-mode operation of neuronal networks involved in left-right alternation. Nature *500*, 85–88.

Tamarkin, D.A., and Levine, R.B. (1996). Synaptic interactions between a muscle-associated proprioceptor and body wall muscle motor neurons in larval and Adult manduca sexta. J. Neurophysiol. *76*, 1597–1610.

Thaëron, C., Avaron, F., Casane, D., Borday, V., Thisse, B., Thisse, C., Boulekbache, H., and Laurenti, P. (2000). Zebrafish evx1 is dynamically expressed during embryogenesis in subsets of interneurones, posterior gut and urogenital system. Mech. Dev. *99*, 167–172.

von der Porten, K., Parsons, D.W., Rothman, B.S., and Pinsker, H. (1982). Swimming in Aplysia brasiliana: analysis of behavior and neuronal pathways. Behav. Neural Biol. *36*, 1–23.

Zarin, A.A., Asadzadeh, J., Hokamp, K., McCartney, D., Yang, L., Bashaw, G.J., and Labrador, J.P. (2014). A transcription factor network coordinates attraction, repulsion, and adhesion combinatorially to control motor axon pathway selection. Neuron *81*, 1297–1311.

Zhang, Y., Narayan, S., Geiman, E., Lanuza, G.M., Velasquez, T., Shanks, B., Akay, T., Dyck, J., Pearson, K., Gosgnach, S., et al. (2008). V3 spinal neurons establish a robust and balanced locomotor rhythm during walking. Neuron *60*, 84–96.